Biocatalytic asymmetric aldol addition into unactivated ketones

Samantha K. Bruffy[1], Anthony Meza[2], Jordi Soler[3], Tyler J. Doyon[1], Seth H. Young[1], Jooyeon Lim[1], Kathryn G. Huseth[2], Marc Garcia-Borràs[3*], Andrew R. Buller[1,2*]

[1]Department of Chemistry, University of Wisconsin−Madison, 1101 University Avenue, Madison, Wisconsin 53706, United States

[2]Department of Biochemistry, University of Wisconsin−Madison, 433 Babcock Drive, Madison, Wisconsin 53706, United States

[3]Institut de Química Computacional i Catàlisi and Departament de Química, Universitat de Girona, C/M. Aurèlia Capmany, 69, 17003 Girona, Spain

*To whom correspondence should be addressed: Marc Garcia-Borràs - Andrew R. Buller (arbuller@wisc.edu)

KEYWORDS: Transaldolase, C–C bond formation, pyridoxal phosphate, tertiary alcohol, non-canonical amino acids, asymmetric catalysis, enzymology

Abstract

Aldolases are prodigious C-C bond forming enzymes, but their reactivity has only been extended past activated carbonyl electrophiles in special cases. We have used a pair of pyridoxal-phosphate-dependent aldolases to probe the mechanistic origins of this limitation. Our results reveal how aldolases are limited by thermodynamically favorable proton transfer with solvent, which undermines aldol addition into ketones. However, we show how a transaldolase can circumvent this limitation by protecting the enzyme-bound enolate from solvent protons and thereby enabling efficient addition into unactivated ketones. The resulting products are non-canonical amino acids with side chains that contain chiral tertiary alcohols. This study reveals the principles for extending aldolase catalysis beyond its previous limits and enables convergent, enantioselective C-C bond formation from simple starting materials.

Researchers have long sought to merge the synthetic utility of high-energy intermediates from traditional organic synthesis with the selectivity of enzyme scaffolds. The past decade has seen dramatic successes with enzymes that use metal-carbenoid[1,2], -nitrenoid[3], and radical type[4,5] intermediates. Carbon-nucleophiles, such as enolates, form the backbone of many synthetic organic methodologies but lack robust biocatalytic counterparts. Aldolases, for example, catalyze C-C bond forming reactions via enolate intermediates and these enzymes have been subjected to decades of engineering, but the scope of electrophiles with which they react is severely limited compared to enolates generated via organic chemistry methods.[6,7] In particular, aldolase-catalyzed additions into ketones, which provide valuable tertiary alcohol products, require either activated ketone substrates or downstream manipulations of the tertiary alcohol product to drive reactions.[8–12] Given the central role of aldolases in biocatalysis, elucidation of principles that enable high-yielding, asymmetric biocatalytic aldol addition into unactivated ketone electrophiles would constitute a major advance.

Here, we use the pyridoxal-phosphate (PLP)- dependent L-threonine aldolases (LTAs) to explore the fundamental limitations of aldolase catalysis. LTAs natively binds L-threonine (Thr) and catalyzes retro-aldol cleavage of the hydroxyethyl side chain, liberating acetaldehyde and a glycyl enolate species that is resonance stabilized by the pyridoxal phosphate cofactor, E(Q^{Gly}) (Fig. S1).[13] This species is then protonated, forming glycine (Gly), which is released into solution. The LTA reaction is reversible and formation of E(Q^{Gly}) by deprotonation of Gly has enabled aldol addition into diverse aldehydes yielding valuable β-hydroxy non-canonical amino acids (ncAAs, Fig. 1A,C).[14] The structure and mechanism of LTAs have been elucidated[15], and these enzymes have been subjected to design efforts,[16] as well as extensive directed evolution campaigns to improve their activity.[17,18] Thus, LTAs represent a mature class of enzymes in biocatalysis.

Despite these efforts, the scope of the Thr aldolases has never been reported to extend beyond aldehydes, reflecting the persistent limitations of aldolase chemistry in biocatalysis. The LTA transformation has a direct counterpart in traditional organic synthesis. Seiple I et al. showed a lithium glycyl enolate bound to a chiral auxiliary can react with diverse ketone electrophiles to access ncAAs bearing chiral tertiary alcohol sidechains,[19] which are found in a variety of bioactive natural products (Fig. 1B).[20–22] The success of this transformation highlights the apparent deficiencies of biocatalysis that, were they overcome, might enable green and efficient routes to chiral tertiary alcohol building blocks.

We began investigating the limitations of aldolase catalysis by challenging the model LTA from *Thermatoga maritima* (*Tm*LTA) to react with an activated trifluoromethyl ketone (TFMK) substrate (**1**). Reactions with 0.1 mol % *Tm*LTA, 100 mM Gly and 10 mM **1** generated the corresponding tertiary alcohol **2** with high stereoselectivity (>30:1 d.r.), albeit in <1% yield (Fig. 1D). Many directed evolution efforts have famously developed highly proficient processes from

such paltry beginnings.[23–25] To assess the potential of directed evolution at improving the reaction, we simulated an enzyme with a higher k_{cat} value by increasing the catalyst loading of *Tm*LTA 10-fold. Despite the increase in catalyst concentration, there was a marginal effect on the yield of the reaction (Fig. 1D,E) and the d.r. underwent rapid decay (Fig. S2), which we attribute to the product reentering the catalytic cycle and scrambling of the imperfectly set β-stereocenter.[14] Whereas faster catalysis had no beneficial effect, increasing the concentration of Gly to 1.0 M, boosted yields to 4%, still falling short of synthetic utility (Fig. S3). Together, these observations are consistent with a reversible reaction that is approaching thermodynamic equilibrium.

High yielding aldol addition into ketones requires overcoming two factors. First, a combination of steric and electronic factors makes ketones upwards of 10^6-fold slower to react than their aldehyde counterparts.[26] Enzymes are renowned for dramatic rate accelerations, however, and these studies with *Tm*LTA demonstrate that the kinetic barrier is surmountable. The second challenge is thermodynamic. Addition into ketones is approximately 10^3 less thermodynamically favorable compared to their aldehyde counterparts. The relative inertness of ketones in organic synthesis is overcome by using high-energy 'kinetic' enolates.[19] In contrast, aldolases in biochemistry, like LTA, form their *C*-nucleophiles through proton transfer with solvent. Irrespective of the diverse molecular mechanisms deployed by aldolases, the energetics of the aldol reaction are thermodynamically linked to C-H deprotonation, as affirmed by a slight shift in equilibrium of the LTA reaction at more acidic pH (Fig S3). Hence, high-yielding aldol addition into even modestly activated ketones cannot occur if the nucleophile is formed through C-H deprotonation without some downstream manipulation of the product, limiting utility.

We hypothesized that a small subgroup of aldolase enzymes, the transaldolases, might be able to overcome these barriers. L-Thr transaldolases (LTTAs) are found in a handful of secondary metabolic pathways.[27–30] Like their counterparts in central metabolism, LTTAs catalyze retro-aldol cleavage of Thr to form E(Q^{Gly}) followed by aldol addition into various aldehyde substrates (Fig. 1A). Previously, we performed mechanistic analysis of a model LTTA from obafluorin biosynthesis.[31] This enzyme, ObiH, has a high kinetic barrier to protonation (Fig. 1C), with a half-life of E(Q^{Gly}) of ~3 h at pH 8.5.[31] Since ObiH does not efficiently engage with proton transfer to bulk solvent, we hypothesized that it may be subject to fundamentally distinct thermodynamic limitations from LTAs. We assayed 0.1 mol % ObiH with 100 mM Thr and 10 mM **1** and, to our delight, observed 25% yield **2** in just 2 h while maintaining high stereoselectivity (Fig. 1D,E). Crucially, higher catalyst loading of ObiH increased the yield, demonstrating the reactions were under kinetic control. To ensure that this reactivity is not limited to the α-aryl acetone motif, which closely mimics the native substrate of ObiH,[29,30] we performed a similar analysis with TFMK **3**. As anticipated, higher catalyst loading of *Tm*LTA did not affect the final yield of reaction with **3**, but increasing the loading of ObiH increased yield with good diastereoselectivity (Fig. 1F). These

data show that the transaldolase reaction of ObiH surpasses the thermodynamic limitations of *Tm*LTA with activated TFMK electrophiles.

Aldol addition into *unactivated* ketones is a distinct challenge, as the starting materials are significantly more stable than TFMKs. Indeed, when *Tm*LTA is challenged with the model ketone **6**, only trace reactivity is observed. Under analogous conditions ObiH catalyzes a productive reaction in 8% yield and high selectivity (Fig. 2A). Increasing the catalyst loading 10-fold did not increase yield (Fig. S4), indicating the reaction achieves equilibrium at low concentrations of tertiary alcohol. Therefore, we sought an additional stratagem to drive reactions to higher yield.

The transaldolase reaction of ObiH generates acetaldehyde as a byproduct of nucleophile formation. We hypothesized that removal of acetaldehyde would further shift the equilibrium of the ObiH reaction to favor product. Beyond a thermodynamic effect, acetaldehyde binds to E(Q^{Gly}) with a K_D of ~400 μM and will act as a competitive inhibitor for alternative electrophiles.[31] Previously, cascade catalysis approaches have been applied to reduce acetaldehyde to drive reactions, including LTTA catalysts with benzaldehydes.[32,33] After reduction of acetaldehyde by alcohol dehydrogenase from *Saccharomyces cerevisiae* (*Sc*ADH), the NADH cofactor can regenerated through the action of the formate dehydrogenase from *Candida boidinii* (*Cb*FDH, Fig. 2B). For ease of use, enzymes were used as clarified lysates. Consistent with our thermodynamic hypothesis, inclusion of the reduction system raised the yield of **21** beyond the previous limits while maintaining high stereoselectivity (Fig. 2A). As each enzyme in this cascade may have different pH optima, we assayed a variety of buffers and found that yields increased when the pH was lowered to 7.0, which we fixed for subsequent experiments (Fig. S5). Increasing the concentration of all proteins slightly increased yields, but lowered d.r.. By only increasing the concentration of *Sc*ADH, both yield and stereoselectivity increased, indicating that a kinetically competitive aldol addition into acetaldehyde was the major factor limiting product formation (Fig. 2C, Fig. S6). When *Tm*LTA was used in place of ObiH in this optimized cascade, low yields were still observed for activated **1**, emphasizing the significance of the kinetic stability of the otherwise identical reactive intermediates (Fig. S7). Crucially, and in contrast to previous methods for driving aldol additions into ketones, this strategy is independent of the tertiary alcohol formed. Consequently, we hypothesized the system could engage with a range of ketone electrophiles.

We measured the total turnover number of ObiH with a variety of ketones on analytical scale using purified ObiH and the reduction system enzymes as clarified lysates (Fig. 2D,E). Using just 0.01 mol % ObiH, reactions with **1** went to quantitative yields and high diastereoselectivity. Additional TFMK substrates **3** and aliphatic **5** underwent ~5000 and ~3500 turnovers, respectfully. Unactivated ketone **6** and heterocyclic analogs **7** and **8** were similarly reactive. Positioning the arene further from the ketone in the form of aryl ether **9** increased reactivity, but decreased diastereoselectivity. Additional unactivated substrates reacted less efficiently, and we

correspondingly increased the catalyst loading of ObiH to 0.05 mol% (Fig. 2E). The ethyl ketone **11** appeared to undergo just 30 turnovers, suggesting a size limit to the binding site of ObiH. Simple acetophenone analogs reacted much less efficiently than the phenylacetones, which mirrors the relative reactivity of the corresponding aldehydes. Acetophenone **12** underwent 120 turnovers but the more activated *p*-NO2 analog **13** underwent just 60 turnovers, which may reflect lower solubility. Only trace activity was observed with ethyl phenyl ketone. The carba-analog of **9** underwent 300 turnovers. Constraining the alkyl moiety in a ring was effective at promoting reactivity. Cyclopentanone **15**, cyclohexanone **16** and cycloheptanone **18** all reacted with superb *ee*. The thia-analog **10** underwent 4000 turnovers. While this ketone does not contain obvious features for electronic activation, higher electrophilicity of this compound was also observed by Cieplak.[34] No reaction was observed with the deactivated cyclohexeneone; additional substrates that did not react are provided in the Supporting Information (Fig. S8). The bulkier aromatic ketone **17** reacted efficiently, but activity was variable due to competing decomposition of the starting material. The bulky, bicyclic tropinone **19** reacted with 160 turnovers. This analytical scope serves to highlight the relative reactivity of diverse ketone substrates.

Using this analytical scale information, we designed preparative scale reactions. Increased concentrations of ketone did not appear to inhibit the enzymes, but yields did not increase commensurately (Fig. S9). We opted to maintain 25 mM ketone with 100 mM Thr as standard conditions for reactions at 1 mmol scale (Fig. 3). TFMK product **2** and **4** reacted efficiently and were isolated in 90% and 80% yield, respectfully, with good to excellent d.r. Reaction with **20**, however showed that removal of an aromatic group reduced activity and diastereoselectivity. The unactivated ketone product **21** was isolated in 43% yield and the corresponding chloro analog **22** in slightly reduced yield and excellent stereoselectivity. The small molecule X-ray structure of **22** confirmed the (2*S*,3*R*) configuration as major. Further substitution of the aryl ring **23-25**, as well as heterocyclic products **26** and **27** were all accessible via this method.

As shown on analytical scale, aryl ether substrates were highly reactive and **28** was isolated in 80% yield. However, the order of the major and minor peaks in the chromatogram was reversed (Fig. S10), affording the possibility of inversion of stereoselectivity at the β-carbon. To assign the absolute configuration, we turned to a biocatalytic resolution of the two diastereomers. We discovered a PLP-dependent phenyl serine dehydratase from *Ralstonia picketti* (*Rpic*PSDH) that was active on the major diastereomer (Fig. S11). Recovery of the minor diastereomer and X-ray crystallography revealed it was the (2*S*,3*R*), 'anti' isomer, indicating that the *syn* isomer is favored.

We hypothesized that the increased activity with the aryl ether of **28** is due to the slight electronic activation of the ketone substrate. Correspondingly, carba- and thioether analogs, **29** and **30**, reacted less efficiently, whereas addition of a remote electron-withdrawing group increased activity and **31** was isolated with good yield and d.r. Isolation of products with cyclic

ketones were more challenging, but we demonstrated **32** in modest yield and superb enantioselectivity via Boc protection.

Comparison of ObiH with its distant homolog *Tm*LTA reinforces the central role of preventing proton transfer from solvent to the unstable E(Q_{Gly}) intermediate. To gain structural insight into the molecular basis for proton transfer within each active site, we turned to constant pH molecular dynamics (CpH-MD) simulations. High-resolution X-ray crystal structures of each enzyme provided a starting point for modelling the dynamics of the E(Q_{Gly}) state. CpH-MD simulations with *Tm*LTA showed formation of an apparent diad between His83, which π-stacks with the pyridine ring, and Asp168, which forms a persistent H-bond with the pyridine N-H (Figure 4). His83 is poised for an efficient water-mediated protonation of the *si*-face of E(Q_{Gly}). There further exists the possibility of *re*-face protonation by Lys199. To experimentally probe the relative reactivity of these protonation pathways, we measured UV-vis spectra of *Tm*LTA bound to L- and D-Ala, which can form an analogous quinonoid intermediate. However, E(Q_{Ala}) was only observed with D-Ala (Fig S12), indicating that proton transfer via the His83-Asp168 diad is the major, most efficient pathway. These residues combine with electrostatic pre-organization of the active site that favor carbanion stabilization at Cα position to effect efficient water-mediated protonation of E(Q_{Gly}) that is essential for the native catalytic cycle of LTAs.

In contrast to *Tm*LTA, CpH-MD simulations of E(Q_{Gly}) formed in ObiH highlighted the absence of such sophisticated proton transfer apparatus to accelerate *si*-face protonation. Due to the H-bond interaction established by Asp204 and protonated E(Q_{Gly}) pyridinium group, E(Q_{Gly}) slightly reorients in the active site and prevents the direct interaction between His131 and Glu109. This avoids the possibility of His131-Glu109 dyad formation and its participation in the activation of a water molecule for the protonation step. A clear molecular strategy for suppressing *re*-face protonation also emerged, as the key catalytic Lys234 residues is sequestered away from the basic Cα position forming an H-bond with the substrate carboxylate and His207 (Figure 4). Throughout our investigation, we had hypothesized that ObiH would have some additional features relative to *Tm*LTA to exclude water from approaching the basic Cα position. Instead, water flowed freely in and out of the active site during simulation. These data provoked us to consider an alternative, simpler hypothesis: proton transfers to conjugated *C*-bases are intrinsically slower due to high re-organization energies.[35,36] In this scenario, the 'kinetic enolate' reactivity of ObiH is not due to some special evolutionary selective pressure, *but rather the absence of one*. Although PLP alone enables slow proton transfer at Cα, these events are nevertheless sluggish, and enzymes must evolve to accelerate them.[37,38] Quantum mechanical calculations of these events are forthcoming.

Conclusions

We have elucidated the factors that have limited aldolase activity in biocatalysis. Nucleophiles that are formed through C-H deprotonation have evolved for fast proton transfer with water, placing intrinsic thermodynamic limitations on their strength. Alternatively, transaldolases form their *C*-nucleophile through C-C bond cleavage. The poorer atom economy of transaldoases may have contributed to a reluctance to explore these enzymes. However, we show formation of persistent, reactive nucleophile can be driven by chemoselective reduction of the aldehyde byproduct. This driving force is independent of the identity of the electrophile and leaves intact the tertiary alcohol products formed. This specific class of ncAAs formed by ObiH were previously accessed through stoichiometric chiral auxiliaries and cryogenic conditions. Correspondingly, this biocatalytic approach provides access to a suite of desirable compounds in a fashion that is amenable to scale. We emphasize this strategy of intermolecular tertiary alcohol formation was enabled not through directed evolution, which cannot overcome thermodynamic barriers, but by careful consideration of enzyme mechanism. With this strategy now clear, protein engineering techniques can be applied to further tailor properties.

Acknowledgements

This work was supported by the Office of the Vice Chancellor for Research and Graduate Education at the University of Wisconsin-Madison with funding from the Wisconsin Alumni Research Foundation and the NIH DP2-GM137417 to A.R.B.; NIH Chemistry−Biology Interface Training Grant T32-GM008505 to A.M.; NIH Biotechnology Training Grant T32-GM008349 to S.H.Y; The Bruker AVANCE III-500 NMR spectrometers were supported by the Bender Fund. M.G.B. thanks the Spanish MICINN (Ministerio de Cienciae Innovación) for PID2019-111300GA-I00 project and the Ramón y Cajal program via the RYC2020-028628-I fellowship. J.S. thanks the Spanish MIU (Ministerio de Universidades) for a predoctoral FPU fellowship FPU18/02380.

References

(1) Coelho, P. S.; Brustad, E. M.; Kannan, A.; Arnold, F. H. Olefin Cyclopropanation via Carbene Catalyzed by Engineered P450 Enzymes. *Science (1979)* **2013**, *339* (6117), 307–310. https://doi.org/10.1126/science.1231434.

(2) Yang, Y.; Arnold, F. H. Navigating the Unnatural Reaction Space: Directed Evolution of Heme Proteins for Selective Carbene and Nitrene Transfer. *Acc Chem Res* **2021**, *54* (5), 1209–1225. https://doi.org/10.1021/acs.accounts.0c00591.

(3) Athavale, S. V.; Gao, S.; Das, A.; Mallojjala, S. C.; Alfonzo, E.; Long, Y.; Hirschi, J. S.; Arnold, F. H. Enzymatic Nitrogen Insertion into Unactivated C-H Bonds. *J Am Chem Soc* **2022**, *144* (41), 19097–19105. https://doi.org/10.1021/jacs.2c08285.

(4) Cheng, L.; Li, D.; Khanh Mai, B.; Bo, Z.; Cheng, L.; Liu, P.; Yang, Y. Stereoselective Amino Acid Synthesis by Synergistic Photoredox-Pyridoxal Radical Biocatalysis. *Science (1979)* **2023**, *381* (6656), 444–451.
(5) Zhou, Q.; Chin, M.; Fu, Y.; Liu, P.; Yang, Y. Stereodivergent Atom-Transfer Radical Cyclization by Engineered Cytochromes P450.
(6) Hélaine, V.; Gastaldi, C.; Lemaire, M.; Clapés, P.; Guérard-Hélaine, C. Recent Advances in the Substrate Selectivity of Aldolases. *ACS Catal* **2022**, *12* (1), 733–761. https://doi.org/10.1021/acscatal.1c04273.
(7) Obexer, R.; Godina, A.; Garrabou, X.; E Mittl, P. R.; Baker, D.; Griffiths, A. D.; Hilvert, D. Emergence of a Catalytic Tetrad during Evolution of a Highly Active Artificial Aldolase. *Nat Chem* **2017**, *9*, 50–56. https://doi.org/10.1038/NCHEM.2596.
(8) Liu, Z. Q.; Xiang, Z. W.; Shen, Z.; Wu, Q.; Lin, X. F. Enzymatic Enantioselective Aldol Reactions of Isatin Derivatives with Cyclic Ketones under Solvent-Free Conditions. *Biochimie* **2014**, *101* (1), 156–160. https://doi.org/10.1016/j.biochi.2014.01.006.
(9) Laurent, V.; Gourbeyre, L.; Uzel, A.; Heíaine, V.; Nauton, L.; Traïkia, M.; Véronique De Berardinis, V.; Salanoubat, M.; Gefflaut, T.; Lemaire, M.; Guérardguérard-Heíaine, C. Pyruvate Aldolases Catalyze Cross-Aldol Reactions between Ketones: Highly Selective Access to Multi-Functionalized Tertiary Alcohols. *ACS Catal* **2020**, *10*, 2538–2543. https://doi.org/10.1021/acscatal.9b05512.
(10) Laurent, V.; Darii, E.; Aujon, A.; Debacker, M.; ean-Louis Petit, J.; HØlaine, V.; ibor Liptaj, T.; Breza, M.; Mariage, A.; Nauton, L.; Traïkia, M.; Salanoubat, M.; arielle Lemaire, M.; hristine GuØrard-HØlaine, C.; de Berardinis, Vø. Biocatalysis Synthesis of Branched-Chain Sugars with a DHAP-Dependent Aldolase: Ketones Are Electrophile Substrates of Rhamnulose-1-Phosphate Aldolases. *Angewandte Chemie International Edition* **2018**, *57*, 5467–5471. https://doi.org/10.1002/ange.201712851.
(11) Maruyama, K.; Miwa, M.; Tsujii, N.; Nagai, T.; Tomita, N.; Harada, T.; Sobajima, H.; Sugisaki, H. Cloning, Sequencing, and Expression of the Gene Encoding 4-Hydroxy-4-Methyl-2-Oxoglutarate Aldolase from Pseudomonas Ochraceae NGJ1. *Biosci Biotechnol Biochem* **2001**, *65* (12), 2701–2709. https://doi.org/10.1271/bbb.65.2701.
(12) Sugiyama, M.; Watanabe, K.; Funakoshi, N.; Amino, Y.; Kawahara, S.; Takemoto, T. Fix Patent, 2002.
(13) Di Salvo, M. L.; Remesh, S. G.; Vivoli, M.; Ghatge, M. S.; Paiardini, A.; D'Aguanno, S.; Safo, M. K.; Contestabile, R. On the Catalytic Mechanism and Stereospecificity of Escherichia Coli l -Threonine Aldolase. *FEBS Journal* **2014**, *281* (1), 129–145. https://doi.org/10.1111/FEBS.12581.
(14) Kimura, T.; Vassilev, V. P.; Shen, G. J.; Wong, C. H. Enzymatic Synthesis of β-Hydroxy-α-Amino Acids Based on Recombinant D- and L-Threonine Aldolases. *J Am Chem Soc* **1997**, *119* (49), 11734–11742. https://doi.org/10.1021/JA9720422.
(15) Di Salvo, M. L.; Remesh, S. G.; Vivoli, M.; Ghatge, M. S.; Paiardini, A.; D'Aguanno, S.; Safo, M. K.; Contestabile, R. On the Catalytic Mechanism and Stereospecificity of Escherichia Coli l -Threonine Aldolase. *FEBS Journal* **2014**, *281* (1), 129–145. https://doi.org/10.1111/FEBS.12581.
(16) Fesko, K.; Uhl, M.; Steinreiber, J.; Gruber, K.; Griengl, H. Biocatalytic Access to α,α-Dialkyl-α-Amino Acids by a Mechanism-Based Approach. *Angewandte Chemie - International Edition* **2010**, *49* (1), 121–124. https://doi.org/10.1002/anie.200904395.

(17) Fesko, K. Threonine Aldolases: Perspectives in Engineering and Screening the Enzymes with Enhanced Substrate and Stereo Specificities. *Appl Microbiol Biotechnol* **2016**, *100*, 2579–2590. https://doi.org/10.1007/s00253-015-7218-5.
(18) Zheng, W.; Yu, H.; Fang, S.; Chen, K.; Wang, Z.; Cheng, X.; Xu, G.; Yang, L.; Wu, J. Directed Evolution of L-Threonine Aldolase for the Diastereoselective Synthesis of β-Hydroxy-α-Amino Acids. *ACS Catal* **2021**, *11* (6), 3198–3205. https://doi.org/10.1021/ACSCATAL.0C04949/SUPPL_FILE/CS0C04949_SI_001.PDF.
(19) Seiple, I. B.; Mercer, J. A. M.; Sussman, R. J.; Zhang, Z.; Myers, A. G.; Seiple, I. B.; Mercer, J. A. M.; Sussman, R. J.; Zhang, Z.; Myers, A. G. Synthetic Methods Stereocontrolled Synthesis of Syn-b-Hydroxy-a-Amino Acids by Direct Aldolization of Pseudoephenamine Glycinamide. *Angewandte Chemie - International Edition* **2014**, *53* (18), 4642–4647. https://doi.org/10.1002/anie.201400928.
(20) Umezawa, K.; Nakazawa, K.; Uemura, T.; Ilccda, Y.; Kondo, S.; Naganawa, H.; Kino, N.; Hashizume, H.; Hamada, M.; Takeuchi, T. Polyoxypeptin Isolated from Streptomyces: A Bioactive Cyclic Depsipeptide Containing the Novel Amino Acid 3-Hydroxy-3-Methylproline. *Tetrahedron Lett* **1998**, *39*, 1389–1392.
(21) Motoyama, T.; Nogawa, T.; Shimizu, T.; Kawatani, M.; Kashiwa, T.; Yun, C. S.; Hashizume, D.; Osada, H. Fungal NRPS-PKS Hybrid Enzymes Biosynthesize New γ-Lactam Compounds, Taslactams A-D, Analogous to Actinomycete Proteasome Inhibitors. *ACS Chem Biol* **2022**. https://doi.org/10.1021/acschembio.2c00830.
(22) Igarashi, M.; Kinoshita, N.; Ikeda, T.; Kameda, M.; Hamadaand, M.; Takeuchi, T. Resormycin, a Novel Herbicidal and Antifungal Antibiotic Produced by a Strain of Streptomyces Platensis I. Taxonomy, Production, Isolation and Biological Properties. *The Journal of Antibiotics* **1997**, *50* (12), 1020–1025.
(23) Crawshaw, R.; Crossley, A. E.; Johannissen, L.; Burke, A. J.; Hay, S.; Levy, C.; Baker, D.; Lovelock, S. L.; Green, A. P. Engineering an Efficient and Enantioselective Enzyme for the Morita-Baylis-Hillman Reaction. *Nat Chem* **2022**, *14* (3), 313–320. https://doi.org/10.1038/s41557-021-00833-9.
(24) Giger, L.; Caner, S.; Obexer, R.; Kast, P.; Baker, D.; Ban, N.; Hilvert, D. Evolution of a Designed Retro-Aldolase Leads to Complete Active Site Remodeling. *Nat Chem Biol* **2013**, *9* (8), 494–498. https://doi.org/10.1038/nchembio.1276.
(25) Savile, C. K.; Janey, J. M.; Mundorff, E. C.; Moore, J. C.; Tam, S.; Jarvis, W. R.; Colbeck, J. C.; Krebber, A.; Fleitz, F. J.; Brands, J.; Devine, P. N.; Huisman, G. W.; Hughes, G. J. Biocatalytic Asymmetric Synthesis of Chiral Amines from Ketones Applied to Sitagliptin Manufacture. *Science (1979)* **2010**, *329* (5989), 305–309. https://doi.org/10.1126/science.1189106.
(26) Li, Z.; Jangra, H.; Chen, Q.; Mayer, P.; Ofial, A. R.; Zipse, H.; Mayr, H. Kinetics and Mechanism of Oxirane Formation by Darzens Condensation of Ketones: Quantification of the Electrophilicities of Ketones. *J Am Chem Soc* **2018**, *140* (16), 5500–5515. https://doi.org/10.1021/jacs.8b01657.
(27) Barnard-Britson, S.; Chi, X.; Nonaka, K.; Spork, A. P.; Tibrewal, N.; Goswami, A.; Pahari, P.; Ducho, C.; Rohr, J.; Van Lanen, S. G. Amalgamation of Nucleosides and Amino Acids in Antibiotic Biosynthesis: Discovery of an L-Threonine:Uridine-5′-Aldehyde Transaldolase. *J Am Chem Soc* **2012**, *134* (45), 18514–18517. https://doi.org/10.1021/ja308185q.

(28) Murphy, C. D.; O'Hagan, D.; Schaffrath, C. Identification of a PLP-Dependent Threonine Transaldolase: A Novel Enzyme Involved in 4-Fluorothreonine Biosynthesis in Streptomyces Cattleya**. *Angew. Chem. Int. Ed* **2001**, *40* (23), 4479–4481.
(29) Schaffer, J. E.; Reck, M. R.; Prasad, N. K.; Wencewicz, T. A. β-Lactone Formation during Product Release from a Nonribosomal Peptide Synthetase. *Nat Chem Biol* **2017**, *13* (7), 737–744. https://doi.org/10.1038/nchembio.2374.
(30) Scott, T. A.; Heine, D.; Qin, Z.; Wilkinson, B. An L-Threonine Transaldolase Is Required for L-Threo-β-Hydroxy-α-Amino Acid Assembly during Obafluorin Biosynthesis. *Nat Commun* **2017**, *8*. https://doi.org/10.1038/ncomms15935.
(31) Kumar, P.; Meza, A.; Ellis, J. M.; Carlson, G. A.; Bingman, C. A.; Buller, A. R. L-Threonine Transaldolase Activity Is Enabled by a Persistent Catalytic Intermediate. *ACS Chem Biol* **2021**, *16* (1), 86–95. https://doi.org/10.1021/acschembio.0c00753.
(32) Xu, L.; Wang, L.-C.; Su, B.-M.; Xu, X.-Q.; Lin, J. Multi-Enzyme Cascade for Improving β-Hydroxy-α-Amino Acids Production by Engineering L-Threonine Transaldolase and Combining Acetaldehyde Elimination System. *Bioresour Technol* **2020**, *310* (April), 123439. https://doi.org/10.1016/j.biortech.2020.123439.
(33) Jones, M. A.; Butler, N. D.; Anderson, S. R.; Wirt, S. A.; Govil, I.; Lyu, X.; Fang, Y.; Kunjapur, A. M. Discovery of L-Threonine Transaldolases for Enhanced Biosynthesis of Beta-Hydroxylated Amino Acids. *Commun Biol* **2023**, *6* (929). https://doi.org/10.1038/s42003-023-05293-0.
(34) Cieplak, A. S. Stereochemistry of Nucleophilic Addition to Cyclohexanone. The Importance of Two-Electron Stabilizing Interactions. *J. Am. Chem. Soc* **1981**, *103* (15), 4540–4552.
(35) Watkins-Dulaney, E. J.; Dunham, N. P.; Straathof, S.; Turi, S.; Arnold, F. H.; Buller, A. R. Asymmetric Alkylation of Ketones Catalyzed by Engineered TrpB. *Angewandte Chemie* **2021**, *133* (39), 21582–21587. https://doi.org/10.1002/ange.202106938.
(36) Costentin, C.; Savéant, J. M. Why Are Proton Transfers at Carbon Slow? Self-Exchange Reactions. *J Am Chem Soc* **2004**, *126* (45), 14787–14795. https://doi.org/10.1021/JA046467H/SUPPL_FILE/JA046467HSI20040615_122542.PDF.
(37) Dixon, J. E.; Bruice, T. C. Comparison of the Rate Constants for General Base Catalyzed Prototropy and Racemization of the Aldimine Species Formed from 3-Hydroxypyridine-4-Carboxaldehyde and Alanine. *Biochemistry* **1973**, *12* (23), 4762–4766. https://doi.org/10.1021/BI00747A031/ASSET/BI00747A031.FP.PNG_V03.
(38) Toth, K.; Amyes, T. L.; Richard, J. P.; Malthouse, J. P. G.; NíBeilliú, M. E. Claisen-Type Addition of Glycine to Pyridoxal in Water. *J Am Chem Soc* **2004**, *126* (34), 10538–10539. https://doi.org/10.1021/JA047501V/ASSET/IMAGES/MEDIUM/JA047501VN00001.GIF.

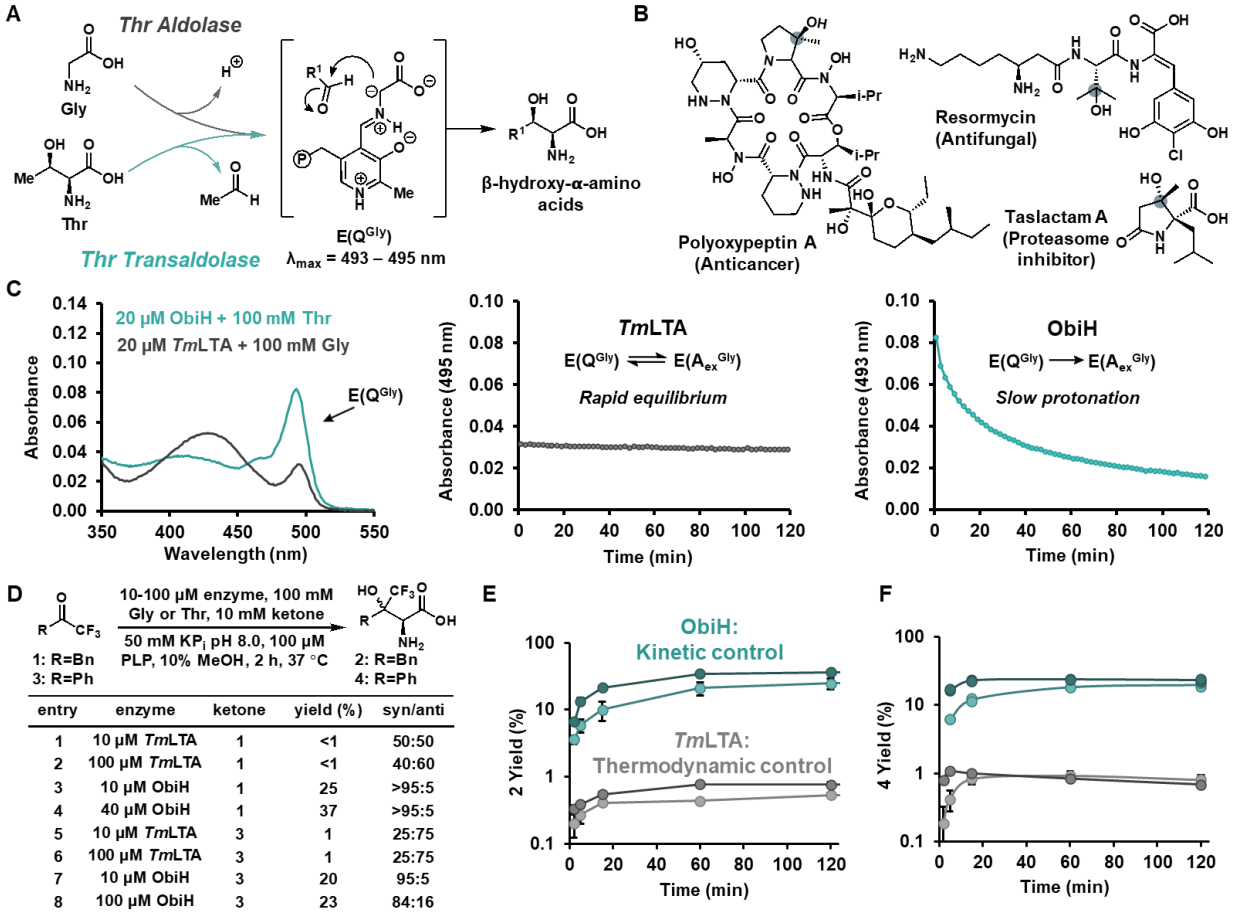

entry	enzyme	ketone	yield (%)	syn/anti
1	10 μM *Tm*LTA	1	<1	50:50
2	100 μM *Tm*LTA	1	<1	40:60
3	10 μM ObiH	1	25	>95:5
4	40 μM ObiH	1	37	>95:5
5	10 μM *Tm*LTA	3	1	25:75
6	100 μM *Tm*LTA	3	1	25:75
7	10 μM ObiH	3	20	95:5
8	100 μM ObiH	3	23	84:16

Figure 1. Kinetic and thermodynamic effects in enzymatic aldol and transaldol reactions. **(A)** Formation of nucleophilic intermediate (E(Q^{Gly})) can occur through two mechanisms, deprotonation at C_α or retroaldol cleavage of Thr sidechain. E(Q^{Gly}) can intercept aldehyde electrophiles to generate β-hydroxy non-canonical amino acids. **(B)** Bioactive natural products bearing tertiary β-hydroxy-α-amino moieties. **(C)** Absorbance spectra of *Tm*LTA (grey) and ObiH (teal) after addition of 100 mM Gly and Thr, respectfully. Monitoring the absorbance of E(Q^{Gly}) at pH = 8.0 over time demonstrates that *Tm*LTA is in rapid equilibrium with protonation, while ObiH is shielded from protonation. **(D)** Yields and diastereomeric ratios of *Tm*LTA and ObiH reactions with activated trifluoromethyl ketones. **(E)** Product formation over time for trifluoromethyl benzyl ketone (**1**) **(F)** Product formation over time for trifluoroacetophenone (**3**). Reactions were conducted with either 10 μM (light grey) or 100 μM (dark grey) *Tm*LTA, or 10 μM (light teal) or 40/100 μM (dark teal) ObiH.

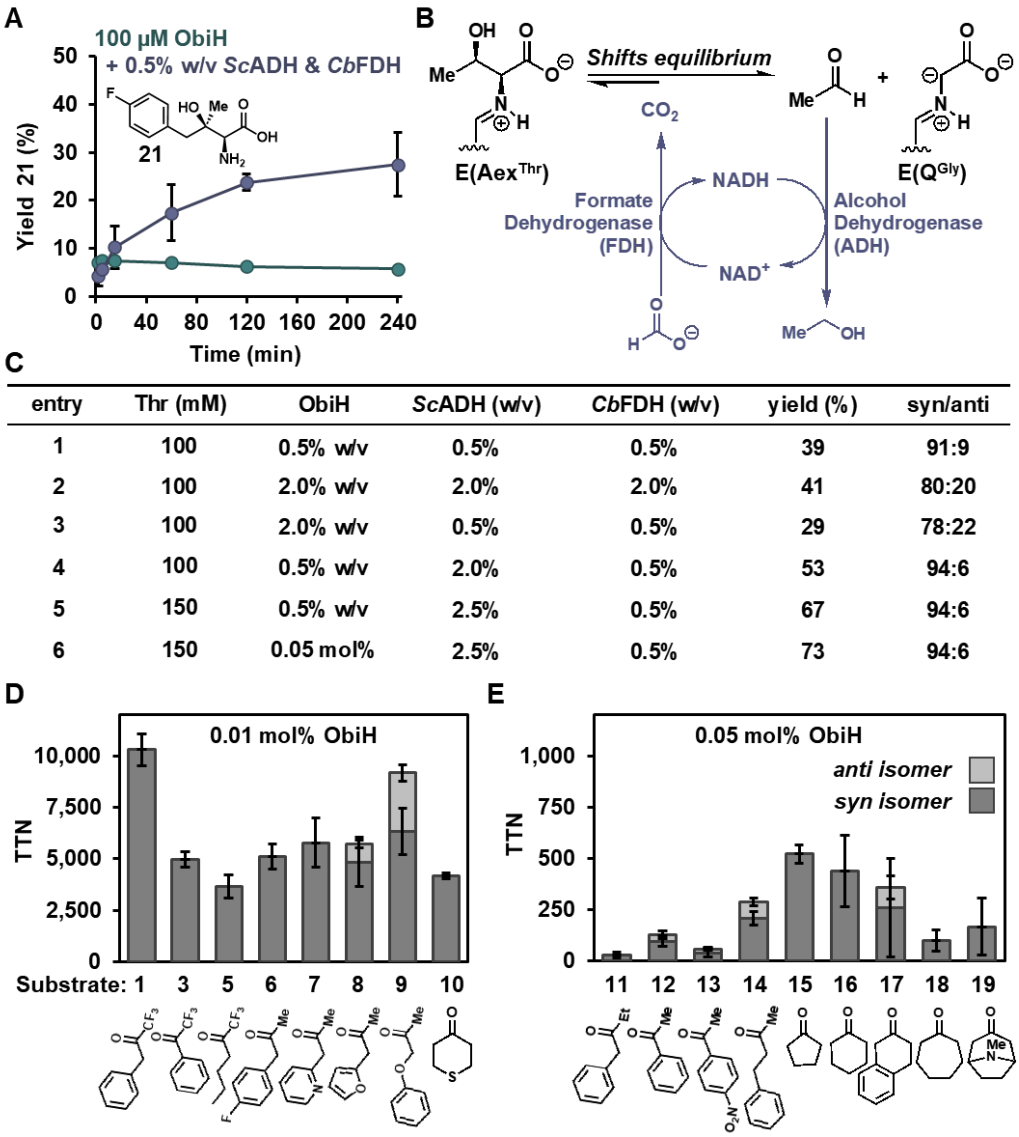

entry	Thr (mM)	ObiH	*Sc*ADH (w/v)	*Cb*FDH (w/v)	yield (%)	syn/anti
1	100	0.5% w/v	0.5%	0.5%	39	91:9
2	100	2.0% w/v	2.0%	2.0%	41	80:20
3	100	2.0% w/v	0.5%	0.5%	29	78:22
4	100	0.5% w/v	2.0%	0.5%	53	94:6
5	150	0.5% w/v	2.5%	0.5%	67	94:6
6	150	0.05 mol%	2.5%	0.5%	73	94:6

Figure 2. Optimization and analytic substrate scope of ObiH with a reduction system. **(A)** Product formation over time for *p*-fluorophenyl acetone (**6**) and ObiH with (purple) or without (black) the reduction system. **(B)** Implementation of an acetaldehyde reduction system adapted from Xu et al. ADH reduces acetaldehyde into ethanol, subsequently shifting the reaction equilibrium to favor generation of the nucleophile, E(Q^{Gly}). The NADH cofactor is regenerated through the action of FDH. **(C)** Optimization of reduction system enzyme's loading concentrations on **5.** Yield and diastereomeric ratios are reported as an average from duplicate reactions. Total turnover number (TTN) were calculated for select ketone substrates using optimized conditions with 0.01 **(D)** or 0.05 **(E)** mol% ObiH. Data points are the average of four individual data points, and the error bars represent the standard deviations from the mean. The relative amount of *syn* isomer to *anti* isomer is designated by different color bars (dark and light grey, respectively).

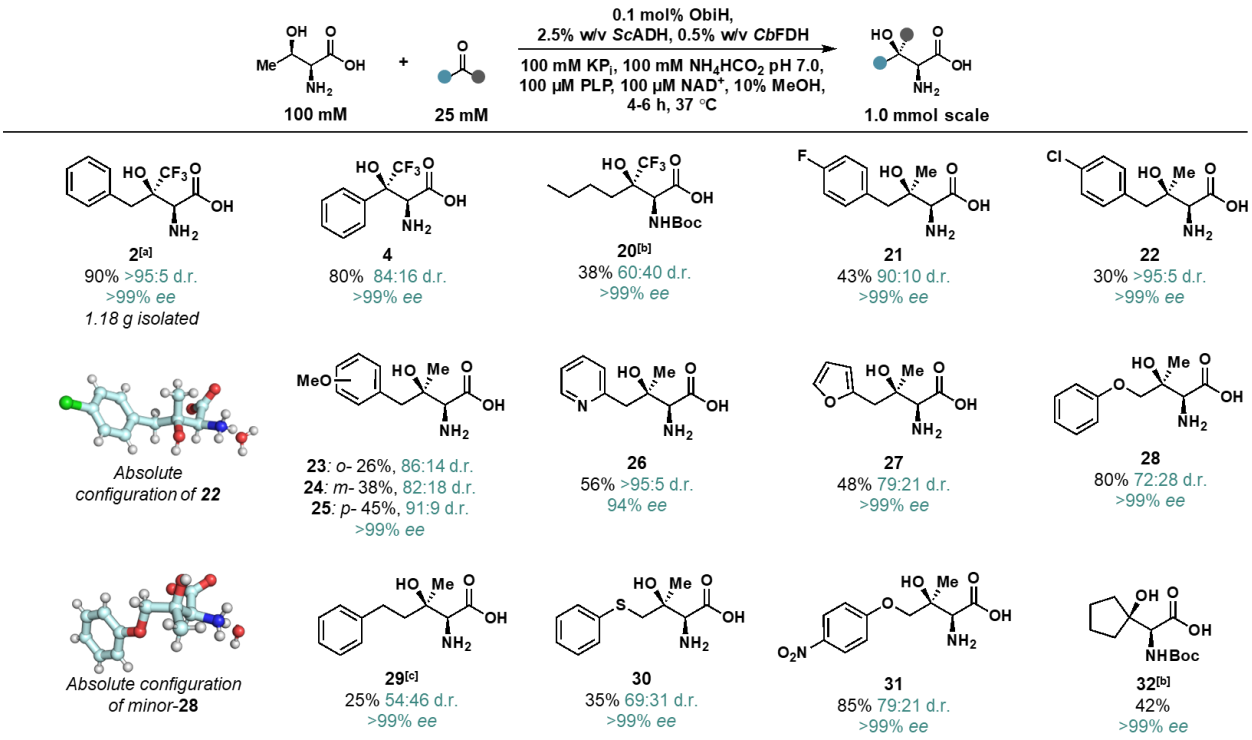

Figure 3. Preparative-scale reactions with ObiH and reduction system. Reactions were conducted with 1 mmol ketone unless otherwise stated. General reaction conditions used 25 mM ketone, 100 mM Thr, 0.1 mol % ObiH, 2.5% w/v *Sc*ADH lysate, 0.5% w/v *Cb*FDH lysate, 100 µM PLP, 100 µM NAD^+, 100 mM KPi buffer pH 7.0, 100 mM ammonium formate, 10% v/v MeOH, 4-6 h, 37 °C. Product purity was assessed via ^1H NMR. All eligible products were derivatized with Marfey's reagent to determine d.r. and %*ee*. [a] The reaction was performed at 5 mmol scale. [b] The products were isolated with Boc-protection. [c] The reaction was performed with 0.4 mol % ObiH.

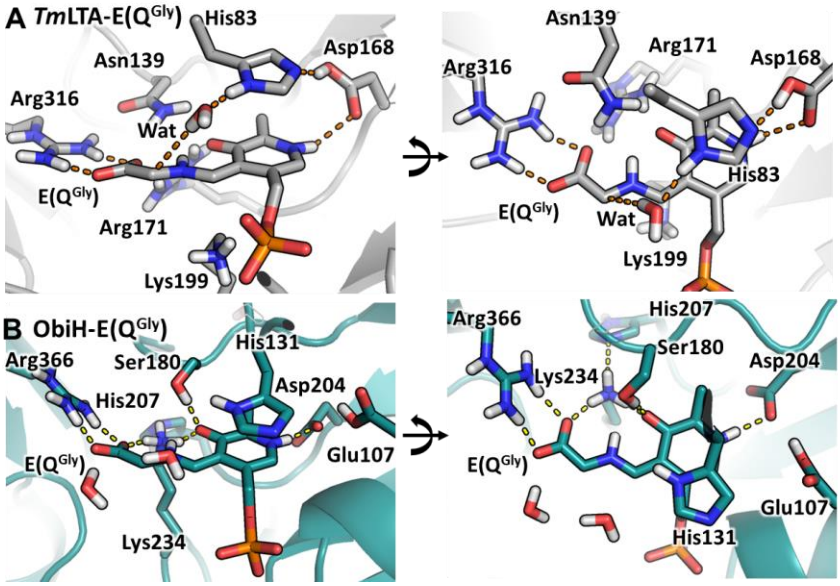

Figure 4. Constant pH molecular dynamic analysis of E(Q^{Gly}) in *Tm*LTA and ObiH. **(A)** In *Tm*LTA, His83 and Asp168 form a catalytic diad poised water-mediated protonation of E(Q^{Gly}). Arg316 forms a salt-bridge with the substrate carboxylate. Lys199 is mobile during simulations. **(B)** In ObiH, His131 does not forms forms no persistent H-bonds during the simulations no water molecules have a persistent orientation conducive to protonation of Cα. Asp204 forms an H-bond with the pyridine N-H and Lys234 is sequestered deep in the active site via H-bonds that include the substrate carboxylate. Select hydrogen bonds are shown via orange dashes.